scientific reports

Check for updates

OPEN

Chrysanthemum morifolium extract improves metabolic dysfunction-associated fatty liver disease by regulating lipid metabolism

Wenjing Yu, Jun Qiu, Yonghu Chen, Xianhua Che✉ & Xuezheng Li✉

Metabolic Dysfunction-Associated Fatty Liver Disease (MAFLD) is one of the most prevalent liver disorders worldwide, yet effective treatment options remain limited. The imbalance between hepatic lipid synthesis and oxidation serves as its primary pathogenic mechanism. The SREBP-1c/FAS/ACCα pathway and PPARα/CPT-1 pathway, acting as key regulators of lipid synthesis and oxidative degradation respectively, play pivotal roles in the development of MAFLD. In this study, we demonstrated that *Chrysanthemum morifolium* (CM) ameliorates liver injury induced by lipid deposition in MAFLD mice, including attenuated steatosis, effective clearance of serum Triglyceride (TG), Total Cholesterol (TC), and low-density lipoprotein (LDL-C), as well as elevated high-density lipoprotein (HDL-C) levels. Further studies showed that among the monomeric compounds isolated from CM lignocellulosic acid (LU), hexaconitine (AR), and lignocellulosic acid-7-O-β-D-glucopyranoside (LU-glu) reduced the lipotropic activity through the SREBP-1c/FAS/ACCα and PPARα/CPT-1 pathways. Overall, our results demonstrate that CM alleviates MAFLD symptoms by inhibiting the SREBP-1c/FAS/ACCα pathway to reduce lipid synthesis while activating the PPARα/CPT-1 pathway to enhance oxidation, thereby maintaining hepatic metabolic homeostasis. This provides a new direction for the development and application of drugs to treat MAFLD.

MAFLD is a prevalent chronic liver disease worldwide, with its incidence showing a significant upward trend in recent years. However, there are currently no specific drugs available for treating MAFLD[1]. The pathogenesis of MAFLD remains unclear to date, with numerous theories proposed. The most widely accepted mechanism is the "two-hit hypothesis" put forward by James et al. based on animal experiment results[2]. The first "hit" centers on insulin resistance, leading to hepatic fat deposition and hepatocellular steatosis[3]. The second "hit" builds upon the initial one, characterized by increased free radicals in the body, mitochondrial oxidative stress, and lipid peroxidation, with certain cytokines causing damage to the liver. According to MAFLD's "two-hit" hypothesis, the occurrence of MAFLD is associated with obesity, steatosis, insulin resistance, etc[4]. Therefore, common MAFLD-related therapeutic drugs primarily target these aspects for treatment. The relevant drugs mainly include lipid-modulating agents, insulin sensitizers, and anti-inflammatory hepatoprotective drugs[5].

The most commonly used lipid-regulating drugs are fibrates and statins, along with other medications such as phosphatidylcholine, orlistat, and sibutramine. According to the MAFLD clinical practice guidelines, statins are effective in reducing low-density lipoprotein cholesterol and serve as a beneficial treatment for preventing cardiovascular diseases, but they do not promote or improve liver conditions[6]. Additionally, increasing phosphatidylcholine intake can enhance hepatic lipid metabolism and reduce MAFLD[7], as phosphatidylcholine participates in the synthesis of very low-density lipoprotein (VLDL) and affects hepatic lipid export. A deficiency in phosphatidylcholine may lead to triglyceride accumulation in the liver. The reversible inhibitors of gastric and pancreatic lipases, orlistat, as well as the norepinephrine and serotonin reuptake inhibitor sibutramine, possess weight-loss and lipid-regulating effects[8]. However, they are no longer recommended for use due to safety concerns.

Insulin sensitizers such as thiazolidinediones and peroxisome proliferator-activated receptor γ agonists (e.g., pioglitazone)[9] can reverse Non-alcoholic steatohepatitis (NASH) and liver fibrosis. The biguanide metformin exhibits both insulin-sensitizing and weight-reducing effects[10]. Said et al. found that metformin showed no significant impact on liver enzymes or histology, making it more suitable for type 2 diabetes patients with MAFLD[11]. Among anti-inflammatory and liver-protective drugs, the antioxidant vitamin E has been reported

College of Pharmacy, Yanbian University Hospital, Yanbian University, Yanji 133002, People's Republic of China. ✉email: sunhwa128@163.com; xzli@ybu.edu.cn

by Hannah W N[12] to improve relevant indicators in NASH patients[13]. The anti-inflammatory and enzyme-lowering drug Cenicriviroc, as a chemokine CCR2/CCR5 antagonist, can suppress inflammation and fibrosis in NASH patients[14]. In summary, due to the unclear pathogenesis of MAFLD and based on currently reported medications, no targeted therapeutic drug suitable for MAFLD has been identified.

A major cause of MAFLD is dysregulation of fatty acid metabolism, involving increased de novo lipogenesis and reduced β-oxidation[15,16]. Under physiological conditions, the synthesis of TG in hepatocytes serves to process excess FFAs. TGs can be stored as lipid droplets within hepatocytes, leading to excessive hepatic TG accumulation, which is associated with increased FFAs supply to the liver from peripheral adipose tissue lipolysis, enhanced de novo lipogenesis, and reduced β-oxidation of FAs[17]. With the continuous deposition of FFAs and cholesterol, related cytokines such as tumor necrosis factor-alpha (TNF-α) and interleukin-6 (IL-6) are activated, exacerbating lipotoxicity and generating reactive oxygen species (ROS), which promotes the progression of MAFLD to NASH, or even liver fibrosis and hepatocellular carcinoma[18]. Therefore, reducing de novo lipogenesis and enhancing oxidative metabolism are crucial for improving MAFLD.

De novo lipogenesis in hepatocytes is primarily regulated by the nuclear transcription factor sterol regulatory element-binding protein 1c (SREBP1c), as well as enzymes such as acetyl-CoA carboxylase (ACC), fatty acid synthase (FAS), and stearoyl-CoA desaturase 1 (SCD1). SREBP1c is activated by insulin and liver X receptor α (LXRα)[19]. Both FAS and ACC1 are downstream target proteins of SREBP1c. In MAFLD, elevated SREBP1c expression stimulates increased expression of FAS and ACC1. FAS serves as the rate-limiting enzyme for long-chain fatty acid synthesis, while ACC1 provides substrates for fatty acid synthesis and simultaneously regulates fatty acid oxidation. The synergistic action of these two constitutes the core engine of de novo lipogenesis (DNL). Increased expression of SREBP1C, ACC1, FAS, and SCD1 promotes hepatic lipid accumulation and induces hepatic steatosis[20]. It is evident that the SREBP-1c/FAS/ACCα pathway plays a pivotal role in lipogenesis and the development of metabolic diseases, serving as a crucial hub connecting nutritional status with cellular lipid homeostasis. In the liver, the overactivation of this pathway is one of the central mechanisms underlying MAFLD.

Another key feature of MAFLD is related to fatty acid oxidative metabolism, which has been identified as a potential therapeutic target for improving MAFLD[21]. Long-chain FAs require activation by carnitine palmitoyltransferase-1 (CPT-1) for membrane transport, whereas short- and medium-chain FAs can cross membranes without activation[22]. CPT-1 is a regulatory enzyme in mitochondria that facilitates the transfer of FAs from the cytosol to mitochondria prior to β-oxidation[23]. In the liver, PPARα plays a crucial role in FA metabolism by upregulating the expression of genes involved in mitochondrial FA and peroxisomal FA oxidation[24]. In addition to regulating metabolic processes, PPARα modulates inflammatory responses by suppressing the expression of inflammatory genes[25]. In MAFLD, decreased PPARα activity leads to insufficient CPT-1 expression, reduced fatty acid oxidation, and hepatic lipid accumulation. The PPARα/CPT-1 pathway serves as the core regulatory axis of fatty acid oxidative metabolism and represents a key therapeutic target for MAFLD. The onset of MAFLD also induces alterations in other related molecular pathways, including inflammatory regulation pathways and cannabinoid receptors (CB1, CB2). For example, TNF-α and IL-6 are two important pro-inflammatory adipocytokines[26,27], which are highly expressed in obese patients and insulin resistance.

Currently, there are no specific therapeutic drugs for MAFLD. The treatment regimen primarily involves lifestyle interventions such as weight loss, a balanced diet, and increased physical activity, while the available pharmacological options remain limited[28]. Modern medical research has demonstrated[29] that CM exhibits hepatoprotective, hypolipidemic, antihypertensive, antioxidant, antitumor, anti-inflammatory, vasodilatory, free radical-scavenging, antibacterial, antiviral, antimutagenic, antiarrhythmic, anti-aging, fatigue-resistant, and lead-eliminating properties. This study aims to explore the effective chemical components in CM that inhibit MAFLD and their potential mechanisms of action, providing a scientific basis for further development and utilization of CM.

Materials and methods

Experimental drug

The flowers of *Chrysanthemum morifolium*(CM) were collected in Tongxiang, Zhejiang Province. China. The plant material was identified by Prof, Guanghai Shen (College of Pharmacy, Yanbian University). A voucher specimen (No.20130719) was deposited in Shenyang Pharmaceutical University Herbarium.

A 95% ethanol extract of CM was subjected to solvent partitioning and subsequently fractionated using various chromatographic techniques, including silica gel column chromatography, polyamide column chromatography, Sephadex LH-20 column chromatography, and preparative thin-layer chromatography. Six compounds (Supplementary Material 1) required for this study were isolated and identified based on their physicochemical properties and spectroscopic data analyses. The ^{1}H NMR spectra are provided in Supplementary Material 2.

Cell culture

The HepG2 cell line purchased from ATCC was cultured in DMEM medium supplemented with 10% fetal bovine serum and 1% streptomycin-penicillin, and maintained at 37 °C with 5% CO_2. Cells were stimulated with different concentrations of mixed free fatty acids (FFAs) at an oleic acid (OA, MW 282.47 g/mol): palmitic acid (PA, MW 256.42 g/mol) ratio of 2:1 (molar ratio) to determine the optimal modeling concentration. Based on this, varying concentrations of CM intervention were subsequently administered.

Preparation of FFAs: mixture to prepare a standardized FFA mixture mimicking physiological serum profiles, OA and PA were combined in a 2:1 molar ratio[30,31]. The acid mixture was dissolved in pre-warmed (70 °C) 0.1 M NaOH solution under vortex oscillation (15 s) to ensure complete solubilization, achieving an initial oleic acid concentration of 100 mM. Subsequently, the solution was diluted with 55 °C pre-warmed 5% defatted BSA to a final oleic acid concentration of 10 mM via vortex mixing (15 s), followed by incubation at 55 °C for 10

min to stabilize FFA-BSA complexes. The mixture was filtered through a 22 μm nylon membrane under sterile conditions to eliminate microbial contaminants, then aliquoted and stored at -20 °C.

Experimental animals

Thirty-two SPF-grade C57BL/6J male mice aged 5 weeks, weighing 22.0 (± 1.8) g, were purchased from Beijing Vital River Laboratory Animal Technology Co., Ltd. After acclimation for one week, the mice were housed in the Animal Care Center of Yanbian University Science Building under controlled conditions (temperature: 23 ± 2 °C, humidity: 60 ± 5%) with a 12-hour light/dark cycle and free access to food and water. Body weight was measured and recorded daily. After the experimental period ended, the animals were exposed to isoflurane and then anesthetized deeply before being euthanized. At the end of the experiment, the animals were placed in isoflurane, followed by deep anesthesia to execute the mice using the decapitation method.

The overall design and protocol of the study were approved by the Laboratory Animal Ethics Committee of Yanbian University (YD20250710023). Animal experiments performed in this study were conducted in accordance with the ARRIVE guidelines (https://arriveguidelines.org), and all methods were performed in accordance with relevant guidelines and regulations.

Grouping and drug administration

After one week of acclimatization, the mice were randomly divided into four groups: the control group, the high-fat diet (HFD) group (model), the low-dose CM group (model + CML 5 mg/mL), and the high-dose CM group (model + CMH 10 mg/mL). The control group was fed with standard chow and received sterilized distilled water (DDW) via gavage, while the other groups were fed with a HFD and administered the corresponding doses of CM via gavage. At 8 and 12 weeks, blood was collected via orbital bleeding, the livers were excised and weighed, and the liver index was calculated.

H&E staining and histological assessment

The liver tissue specimens fixed with 4% formaldehyde were used for pathological examination of liver tissue. After sequential dehydration with gradient ethanol, paraffin embedding was performed using a paraffin embedding machine (Thermo, USA). The wax blocks were sectioned into 5 μm slices and baked at 60 °C for 6 h. The sections were dewaxed with xylene, washed with gradient ethanol, and rinsed with PBS. The samples were stained with H&E staining (APExBIO, USA) strictly following the H&E staining protocol. The sections were mounted with neutral resin (Solarbio, China) and observed under an optical microscope (Olympus Corporation, Japan). Liver histology was evaluated according to the NAFLD Activity Score (NAS) system (steatosis, 0–3; lobular inflammation, 0–3; hepatocyte ballooning, 0–2; total score, 0–8), with fibrosis staged separately. All sections were independently assessed in a blinded manner by two experienced pathologists; in cases where the scores differed by ≥ 2 points, a third pathologist reviewed the slides and the final score was determined either by consensus or by taking the median value. Lobular inflammatory foci were quantified at 200× magnification, with each sample evaluated across the whole section and both the highest and average field counts recorded[32]. The assessment of hepatocyte ballooning was performed in accordance with the criteria proposed by Kleiner et al.[33].

Determination of TG, TC HDL-C and LDL-C levels

Mouse serum was collected, and the levels of TG, TC, HDL-C and LDL-C in the serum were measured according to the instructions of the TG, TC, HDL-C and LDL-C assay kits.

MTT assay

Except for the control group, the remaining groups were administered drugs according to the experimental design and cultured for 24 h to allow drug action. MTT was then added and cultured in the dark for 2 h. After dissolution, the medium was aspirated under dark conditions, and 100 μL of analytically pure DMSO was added to each well to dissolve the formazan crystals. The OD value was measured at 490 nm. Data were processed to calculate cell survival rates.

Oil red O staining

Place specialized round cell glass coverslips on the bottom of a 6-well plate, then culture the cells at 37 °C with 5% CO_2 for 18 h until a confluent monolayer forms. Administe treatments according to the experimental design and incubate for 24 h to allow drug action. After treatment, transfer the coverslips onto microscope slides with water sealing for observation and photography under a microscope. Remove the coverslips and fully dissolve the Oil Red O stain using 200 μL pure isopropanol. Transfer the solution to a 96-well plate, adding 100 μL of the Oil Red O eluate per well. Measure the OD values at 450 nm wavelength and generate bar graphs to compare the relative Oil Red O content between groups.

RT-qPCR

According to the experimental design, cells were grouped and administered with drugs, then cultured for 24 h to allow drug action. Total mRNA was extracted and dissolved in an appropriate amount of DEPC water, followed by incubation at a constant temperature of 72 °C for 10 min. Reverse transcription was performed, and after quantification using a microplate reader, a 20 μL system was prepared according to the instructions of the reverse transcription kit. cDNA was synthesized using a PCR machine. For PCR amplification, a 20 μL system was prepared according to the SYBR Green PCR Kit instructions, and amplification and fluorescence quantification of related gene levels were conducted using a Real-Time PCR instrument. For data processing, after exporting data from the RT-PCR system, relative quantitative analysis of mRNA expression levels of SREBP-1c, FAS, and PPARα was performed according to the specified formula.

Western blot

Cells treated according to the experimental design were collected in ice, centrifuged, and quantified by BCA method. Polyacrylamide gels were electrophoresed and transferred to NC membranes. Closure was performed using 5% skim milk powder or 5% bovine serum albumin. Primary antibodies were added dropwise overnight at 4 °C, including β-Actin (8H10D10) Mouse mAb (Cell Signaling), FAS (4C3) Mouse mAb (Cell Signaling), Anti-PPAR alpha (phosphoS12) antibody (Abcam), CPT1 Polyclonal Antibody (ABclonal), HMGCR Polyclonal Antibody (ABclonal), TNF-alpha Polyclonal Antibody (ABclonal), p-ACC alpha (SANTA CRUZ), ACC alpha (SANTA CRUZ), ATGL (SANTA CRUZ). After washing, they were immersed in secondary antibody orking solution (1:20000, LI-COR Biosciences). Processing was visualized using a dual-color infrared laser imaging system (LI-COR Odyssey Clx, USA) and analyzed using ImageJ 8.0.

ELISA

Serum lipopolysaccharide (LPS) levels in mice were measured using an ELISA kit (Excell Bio, Jiangsu, China) according to the manufacturer's instructions. Concentrations were determined by comparing the optical density values at 450 nm with the corresponding standard curve.

Measurement of MDA and SOD in liver tissue

Mouse liver tissues were homogenized in PBS at a ratio of 1:10 (w/v). Changes in oxidative stress–related markers in the liver homogenates were assessed using the corresponding kits according to the manufacturer's instructions (Jiancheng Bioengineering Institute, Nanjing, China).

Measurement of serum lipids and transaminases

Serum levels of triglycerides (TG), total cholesterol (TC), high-density lipoprotein cholesterol (HDL-C), low-density lipoprotein cholesterol (LDL-C), alanine aminotransferase (ALT), and aspartate aminotransferase (AST) were measured using the respective assay kits (A110-1, A111-1-1, A113-1-1, A112-1-1, C009-2-1, and C010-2-1; Jiancheng Bioengineering Institute, Nanjing, China) according to the manufacturer's instructions.

Statistical analysis

Data were statistically analysed and graphed using GraphPad Prism 7.0. At least three sets of data were collected from each experiment and are expressed as means ± standard deviation. The significance level of the differences between the groups was analyzed through one-way or two-way analysis of variance or paired t-tests.

Results

Hypolipidemic activity of CM ethanol total extract in ameliorating MAFLD in mice

To investigate whether the total ethanol extract of CM could alleviate MAFLD symptoms, a HFD-induced MAFLD mouse model was established. Analysis of body weight revealed that, compared with the control group, the body weight of model mice increased significantly from 4 weeks onward and continued to rise throughout the experiment (Fig. 1A). In contrast, both CML and CMH interventions markedly attenuated body weight gain, while no significant differences in liver index were observed among groups (Fig. 1B). Regarding serum biochemical parameters, the model group exhibited significantly elevated levels of TG, TC, LDL-C, and IDL-C (Fig. 1C, F-H), whereas CML and CMH treatments significantly reduced these levels, with CMH exerting more pronounced effects.

Histological analysis by HE staining demonstrated that, at 4 weeks, livers from the model group displayed evident lipid vacuole formation, predominantly microvesicular and medium-sized steatosis, accompanied by mild inflammatory cell infiltration. By week 8, hepatic steatosis was further aggravated, with large lipid droplets and marked inflammatory responses, which resulted in a significantly elevated NAS score (Fig. 1D, E). In contrast, CM treatment notably reduced both the number and size of lipid vacuoles and alleviated inflammation at both 4 and 8 weeks, while CMH exerted stronger protective effects, with relatively preserved hepatic architecture, only a few scattered lipid droplets, and markedly reduced inflammation. Accordingly, NAS scores in the CML and CMH groups were significantly lower than those in the model group.

Furthermore, serum ALT and AST levels were markedly elevated in the model group (Fig. 1I, J), indicating hepatic injury, whereas both CML and CMH treatments significantly improved liver function. Consistently, hepatic TG levels were markedly elevated in the model group but were significantly reduced following CML and CMH intervention (Fig. 1K). Collectively, these findings indicate that CM, particularly at high dosage, exerts pronounced protective effects against HFD-induced lipid metabolic disorders and liver injury.

In summary, CM exhibited significant lipid-lowering activity in vivo. To further elucidate its mechanism of action, we conducted component isolation of CML to obtain its primary chemical constituents and evaluated their lipid-lowering effects using *in vivo and in vitro* models.

Total ethanol extract of CM reduces lipid accumulation in vivo by inhibiting lipogenesis and enhancing fatty acid oxidation

Since MAFLD progression is driven not only by lipid metabolic disorders but also by inflammation, oxidative stress, and gut microbiota dysbiosis, we first evaluated the effects of CM on hepatic inflammation and oxidative stress, followed by its influence on lipid metabolism. Compared with controls, model mice exhibited markedly increased hepatic IL-1β and IL-6 mRNA expression (Fig. 2A, B), decreased SOD activity, and elevated MDA and serum LPS levels (Fig. 2C-E), reflecting hepatic inflammation, oxidative stress, and impaired gut barrier function. CM administration significantly ameliorated these alterations, with CMH showing the most pronounced effects.

To further evaluate the effects of CM on lipid metabolism pathways, western blot analysis was performed. The results indicated that the model group exhibited upregulated expression of FAS and HMGCR, along with

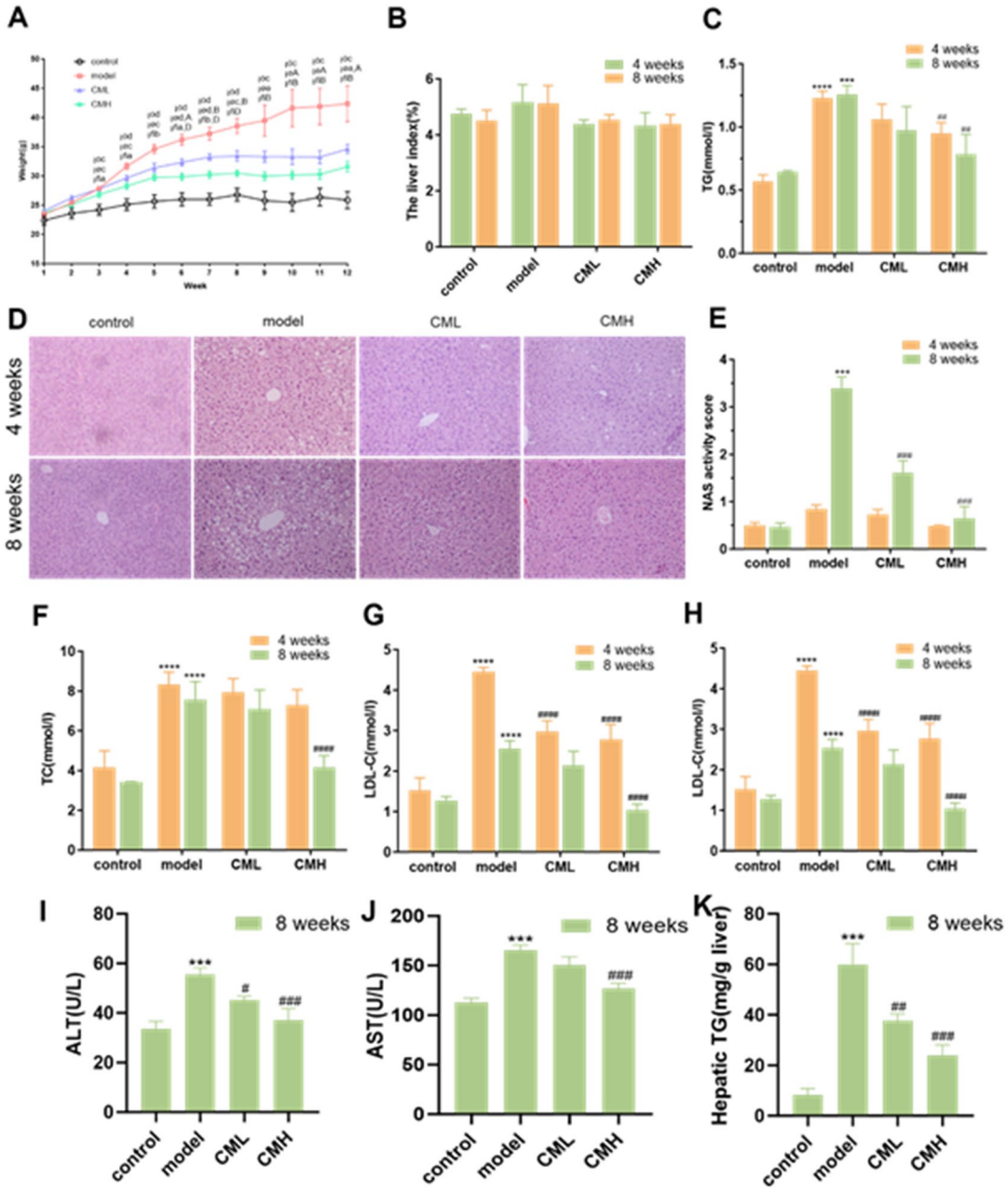

Fig. 1. CM ethanol extract improves lipid-lowering activity in MAFLD mice. (**A**) Body weight changes (compared with normal group: $^{a}P<0.05$, $^{b,c,d}P<0.01$; compared with model group: $^{A}P<0.05$, $^{B,C,D}P<0.01$). (**B**) Liver index of mice. (**C,F–H**) Serum lipid content in mice. (**D**) HE staining results of liver paraffin sections in mice). **E.** Quantification of NAS activity score. (**I**, **J**) Serum ALT and AST levels in mice. (**K**) Hepatic TG content in mice. (compared with control group: $^{*}P<0.05$, $^{**}P<0.01$, $^{***}P<0.001$; compared with model group: $^{\#}P<0.05$, $^{\#\#}P<0.01$, $^{\#\#\#}P<0.001$).

downregulated expression of PPARα and CPT-1 (Fig. 2F, G), suggesting enhanced hepatic lipogenesis and suppressed fatty acid oxidation. CM treatment significantly reversed these alterations, characterized by decreased FAS and HMGCR levels and increased PPARα and CPT-1 expression.

In summary, CM effectively ameliorates hepatic inflammation, oxidative stress, and lipid metabolic disorders in model mice, with the protective effects being more prominent in the CMH group.

Total ethanol extract of CM demonstrates effective lipid-lowering in vitro

To further screen for effective lipid-lowering components in CM, an in vitro model of MAFLD was established using the human hepatocellular carcinoma HepG2 cell line induced by FFAs. The development of a cell model that effectively mimics lipid accumulation is of significant importance for advancing research into the mechanisms of MAFLD and for developing effective prevention and treatment strategies. Due to advantages

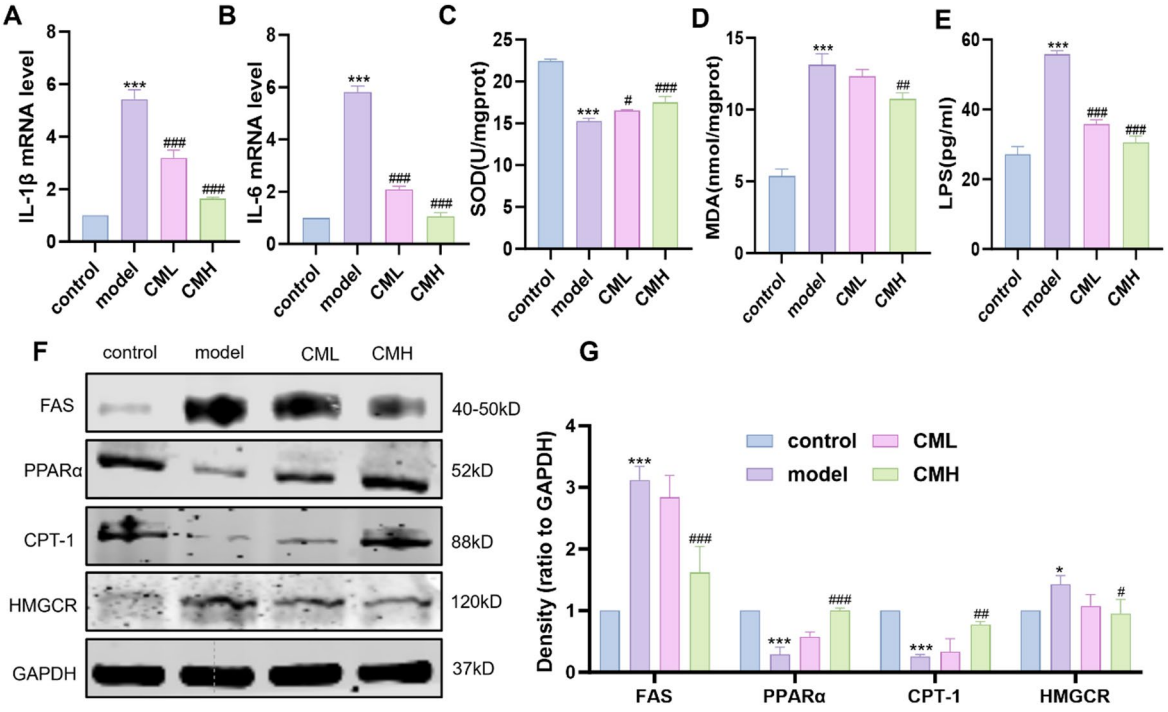

Fig. 2. Total ethanol extract of CM reduces lipid accumulation in vivo by inhibiting lipogenesis and enhancing fatty acid oxidation. (**A**, **B**) RT-qPCR analysis of hepatic mRNA expression levels of IL-1β and IL-6 in mice. (**C**–**E**) Serum levels of MDA, SOD, and LPS in mice. (**F**, **G**) Western blot analysis of hepatic protein expression of ATGL, PPARα, CPT-1, and HMGCR (compared with control group: $^{*}P<0.05$, $^{**}P<0.01$, $^{***}P<0.001$; compared with model group: $^{\#}P<0.05$, $^{\#\#}P<0.01$, $^{\#\#\#}P<0.001$).

such as shorter experimental cycles, high reproducibility, and operational convenience, in vitro cell models induced to exhibit lipid accumulation have become a vital approach in studying this disease. Specifically, FFAs—typically a combination of OA and PA are applied to hepatocyte lines (e.g., HepG2). This treatment effectively simulates a state of lipid metabolism disorder observed in vivo, triggering intracellular lipid accumulation, cell damage, and inflammatory responses, which represent typical pathological processes of MAFLD.

First, we examined the cell viability after intervention with CM ethanol total extract (Fig. 3A) and FFAs (Fig. 3B) in HepG2 cells. The results showed significant cellular inhibition when the concentration of CM ethanol total extract reached 50 μg/mL and FFAs reached 800 μmol/L. Subsequently, TG levels (Fig. 3C) served as the primary indicator, supplemented by Oil Red O staining experiments (Fig. 3E, F), to confirm hepatic steatosis and further validate the establishment of the FFAs-induced MAFLD model in HepG2 cells. After FFAs intervention, TG content continuously increased with rising FFAs concentrations. Oil Red O staining also demonstrated that intracellular lipids progressively accumulated with higher FFAs concentrations, the results indicate that the MAFLD cell model was successfully constructed. Based on these experimental results, this study adopted 400 μmol/L FFAs for subsequent experiments. Next, we treated the MAFLD in vitro model with different concentrations of CM ethanol total extract, using Fenofibrate (Feno) as the positive control. The results showed that when CM ethanol total extract reached 10 μg/mL, TG content significantly decreased compared to the model group. At 20 μg/mL concentration, the lipid-lowering effect became comparable to the Feno group (Fig. 3D). The Oil Red O staining assay (Fig. 3G, H) demonstrated that dissolved Oil Red O dye entered the cells. When the CM group concentration reached 20 μg/mL, HepG2 intracellular lipid content showed significant reduction compared to the model group. At 40 μg/mL concentration, the lipid-lowering effect was comparable to Feno.

In summary, we have verified that CM also exhibits significant lipid-lowering activity in the in vitro MAFLD model. The next step will involve intervening in the in vitro MAFLD model using the major compounds isolated from CM to investigate the effects of these monomeric compounds derived from CM on MAFLD.

CM monomer compounds to enhance lipid-lowering activity in vitro

None of the six monomer compounds in CM were toxic to HepG2 cells at a concentration of 30 μmol/L. In the later in vitro experiments of monomer compounds affecting MAFLD, an initial screening was performed using a concentration setting of 30 μmol/L (Fig. 4A). Detection of TG content revealed (Fig. 4B) that except for Apigenin (AP), the five monomer compounds intervening in the MAFLD model significantly reduced the TG content in comparison with the model group, with LU, Artemisetin (AR), LU-glu, and Salicylic acid (SA) achieving 40%, 43%, 50%, and 61% reduction in TG, respectively. It indicated that most of the isolated monomer compounds obtained from CM exhibited TG-lowering activity. Oil red O staining experiments showed (Fig. 4C, D) that the volume of intracellular lipid droplets decreased after the intervention of monomer compounds from CM in the

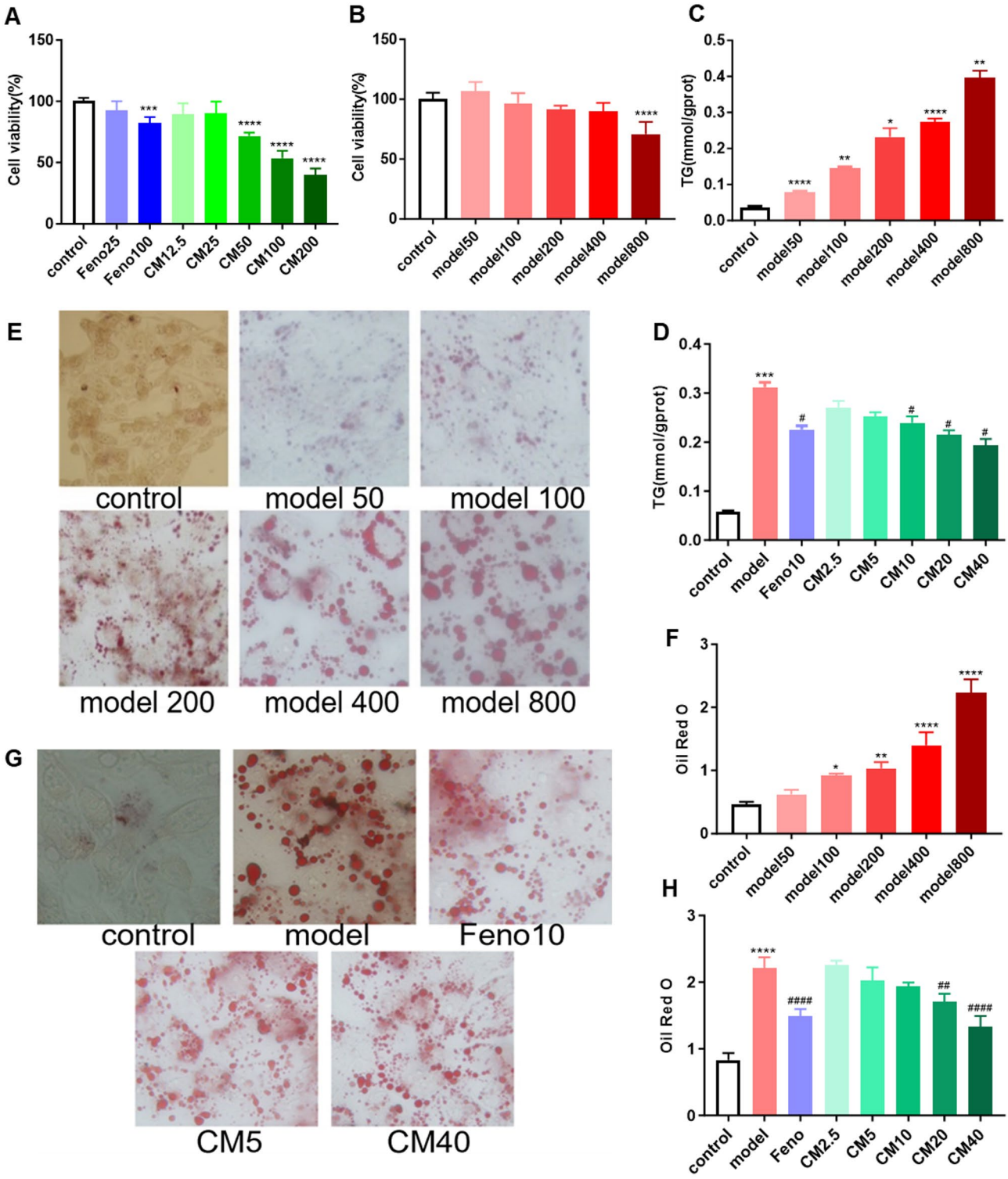

Fig. 3. CM has significant lipid-lowering activity in an in vitro MAFLD model. (**A**) Effect of total CM ethanol extracts on HepG2 cell survival (**B**) Effect of FFAs on HepG2 cell survival (**C**) Effect of FFAs on TG content of HepG2 cells. (**D**) Effect of CM ethanol total extracts on TG content in an MAFLD model. (**E**, **F**) Effect of FFAs on oil red O staining and its relative content in an in vitro model of MAFLD. (**G**, **H**) Effect of total CM ethanol extracts on oil red O staining and its relative content in an in vitro model of MAFLD (compared with normal group: $^{*}P<0.05$, $^{**}P<0.01$, $^{***}P<0.001$, $^{****}P<0.0001$; compared with model group: $^{\#}P<0.05$, $^{\#\#}P<0.01$, $^{\#\#\#}P<0.001$, $^{\#\#\#\#}P<0.001$).

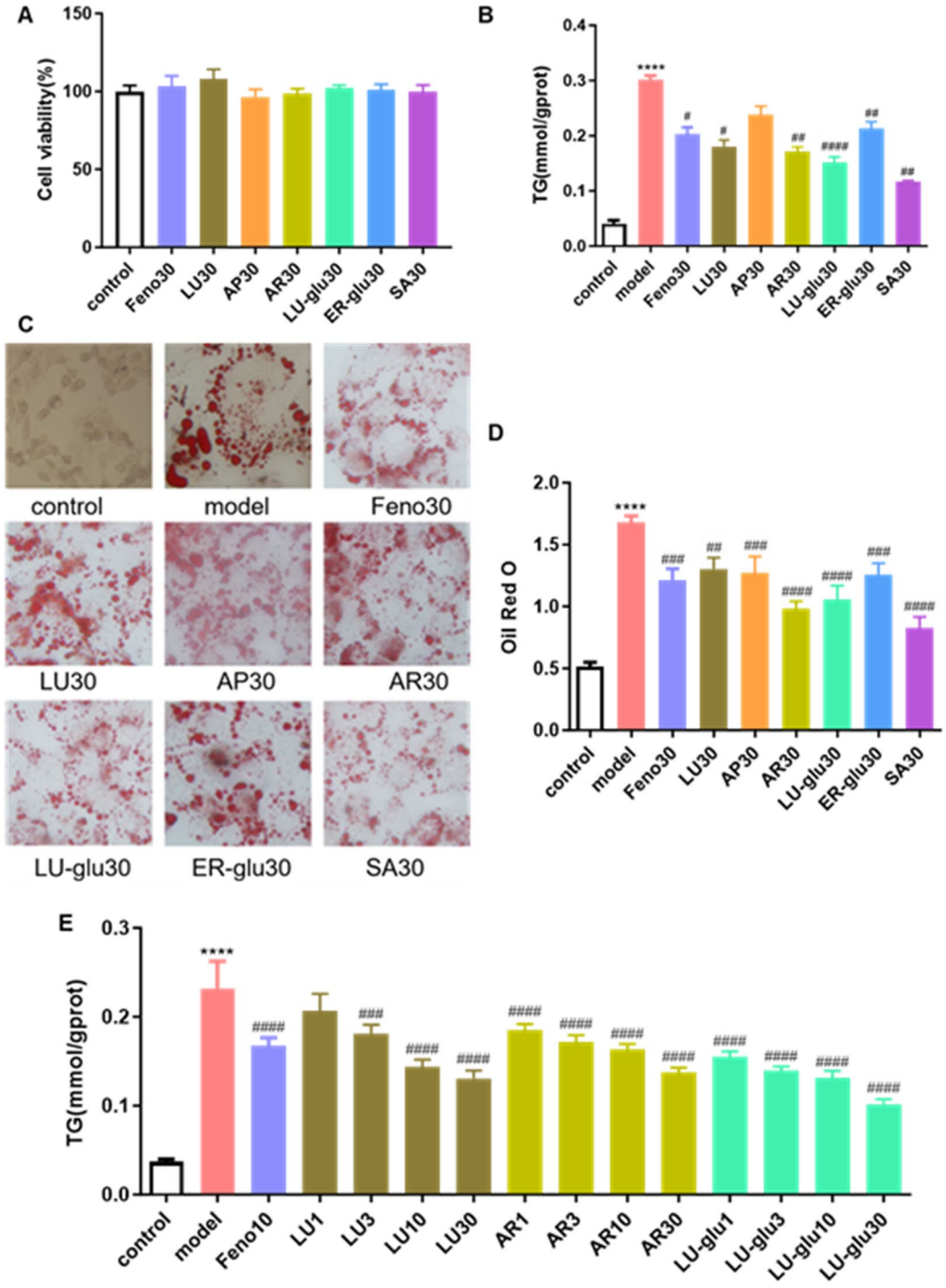

Fig. 4. CM monomer compounds to enhance lipid-lowering activity in vitro. (**A**) Effect of monomer compounds in CM at 30 μmol/L on the survival of HepG2 cells (**B**) Effect of monomer compounds at 30 μmol/L on TG content in an in vitro model of MAFLD. (**C**, **D**) Effect of CM monomer compounds on oil red O staining and its relative content in an in vitro model of MAFLD. (**E**) Effects of LU, AR, and LU-glu on TG content in the in vitro model of MAFLD (compared with normal group: $^{*}P<0.05$, $^{**}P<0.01$, $^{***}P<0.001$, $^{****}P<0.0001$; compared with model group: $^{\#}P<0.05$, $^{\#\#}P<0.01$, $^{\#\#\#}P<0.001$, $^{\#\#\#\#}P<0.001$).

MAFLD in vitro model compared with the staining map of the model group, and the relative content measured by dissolution staining into oil red O. Each monomer compound group showed a significant reduction in lipid content compared with the model group.

Combining the above experimental results, LU, AR, LU-glu and SA have significant lipid-lowering activity, and SA is a more common compound with lipid-lowering effect, so in this study, we selected LU, AR and LU-glu for further lipid-lowering in vitro model and the related mechanism study. We set up different concentrations

of the above three monomer compounds to intervene in the in vitro MAFLD model for the study (Fig. 4E), and further measured the TG values of the three compounds at different concentrations after intervention in the MAFLD in vitro model, which fully confirmed the good lipid-lowering effects of LU, AR, and LU-glu, and the three monomers had a significant TG-lowering effect at a concentration of 3 μmol/L. The three monomers had significant TG-lowering effects at a concentration of 3 μmol/L. The three monomers had significant TG-lowering effects in the in vitro model. So far, this part of the experiment focused on the screening of monomer compounds to obtain monomer compounds with significant lipid-lowering activity, and combined with CM itself as a traditional Chinese medicine, three of the monomer compounds, LU, AR, and LU-glu, were selected to continue the third part of the lipid-lowering related mechanism investigation.

LU, AR, and LU-glu ameliorate MAFLD and inhibit deterioration in terms of reduced lipid synthesis

Through the screening of the above experiments, we compared LU, AR, and LU-glu with more prominent lipid-lowering effects. We further used RT-qPCR and Western blot to detect the mRNAs of SREBP-1c, FAS, PPARα, and the expression levels of FAS, a type of regulatory lipid synthesis protein, after the intervention of the three compounds at different concentrations in the MAFLD model of HepG2 cells expression levels.

RT-qPCR results showed that in the model group, the mRNA levels of SREBP-1c and FAS, both of which regulate lipid synthesis from scratch, were significantly increased, and the mRNA level of PPARα, which regulates lipids undergoing β-oxidation, was significantly decreased (Fig. 5A); all three compounds, LU, AR, and LU-glu, reversed the trend of SREBP-1c and PPARα, and AR and LU-glu also significantly decreased the level of FAS, which regulates lipid synthesis from scratch (Fig. 5C, D). LU-glu also significantly reduced the mRNA level of FAS (Fig. 5B), which was consistent with the western blot results; in addition, the phosphorylation level of ACCα protein was up-regulated in the model group(Fig. 5E, F), showing an increase in lipid synthesis, and the intervention of LU, AR, and LU-glu significantly reduced the level of phosphorylated ACCα, which locus reduced the ab initio synthesis of lipids.

LU, AR and LU-glu improve MAFLD and inhibit deterioration from enhanced oxidation and other aspects

We then examined the expression levels of mRNA and phosphorylated ACCα, PPARα, CPT-1, ATGL, HMGCR, which are lipid oxidation-related proteins, as well as TNF-α for the three compounds PPARα.

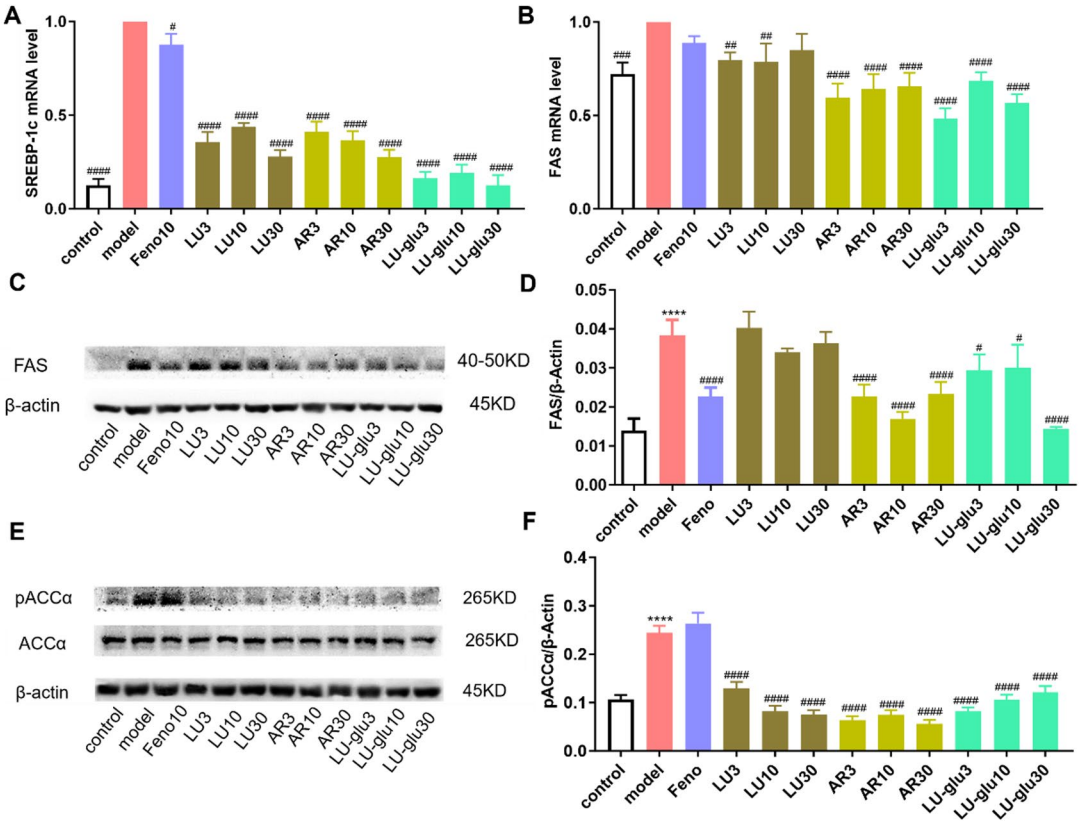

Fig. 5. LU, AR, and LU-glu ameliorate MAFLD and inhibit deterioration in terms of reduced lipid synthesis. (**A**, **B**) RT-qPCR to detect the mRNA expression levels of SREBP-1c, FAS (**C**–**F**) Western blot to detect lipid synthesis-related protein bands (compared with normal group: $^{*}P<0.05$, $^{**}P<0.01$, $^{***}P<0.001$, $^{****}P<0.0001$; compared with model group: $^{\#}P<0.05$, $^{\#\#}P<0.01$, $^{\#\#\#}P<0.001$, $^{\#\#\#\#}P<0.001$).

In terms of lipid oxidation, the expression of PPARα and CPT-1 (Fig. 6B-D) was significantly downregulated in the model group, leading to impaired oxidation and lipid accumulation. Treatment with LU, AR, and LU-glu markedly upregulated PPARα expression, exceeding that of the positive control fenofibrate, consistent with the RT-qPCR results (Fig. 6A). Notably, all three compounds restored the expression of PPARα and CPT-1, thereby enhancing lipid oxidation.

Regarding other lipid-related factors, ATGL (Fig. 6E, G) serves as the rate-limiting enzyme in TG hydrolysis, regulating the breakdown of TG[34]. In contrast to some studies, our results showed that ATGL protein levels were elevated in the model group; however, hepatic triglyceride accumulation remained significant. This suggests that increased ATGL expression does not necessarily translate into enhanced lipolytic activity. Previous studies have demonstrated that the lipolytic function of ATGL is highly dependent on its co-activator CGI-58. Under pathological conditions such as fatty liver, CGI-58 is competitively bound by proteins such as PNPLA3, thereby attenuating its activation of ATGL[35,36]. In addition, proper lipid droplet localization and membrane trafficking are also critical for ATGL function. Dysregulation or loss of regulatory proteins (e.g., STX11) can lead to elevated ATGL expression without effective catalytic activity[37]. Therefore, we speculate that the upregulation of ATGL observed in model mice is more likely a compensatory response; however, impaired cofactor availability or localization mechanisms prevent a functional increase in lipolysis, ultimately resulting in persistent TG accumulation. Importantly, unlike the other two compounds, LU-glu appears to regulate both ATGL expression and its associated regulatory mechanisms, thereby restoring TG hydrolysis. This mechanistic effect is consistent

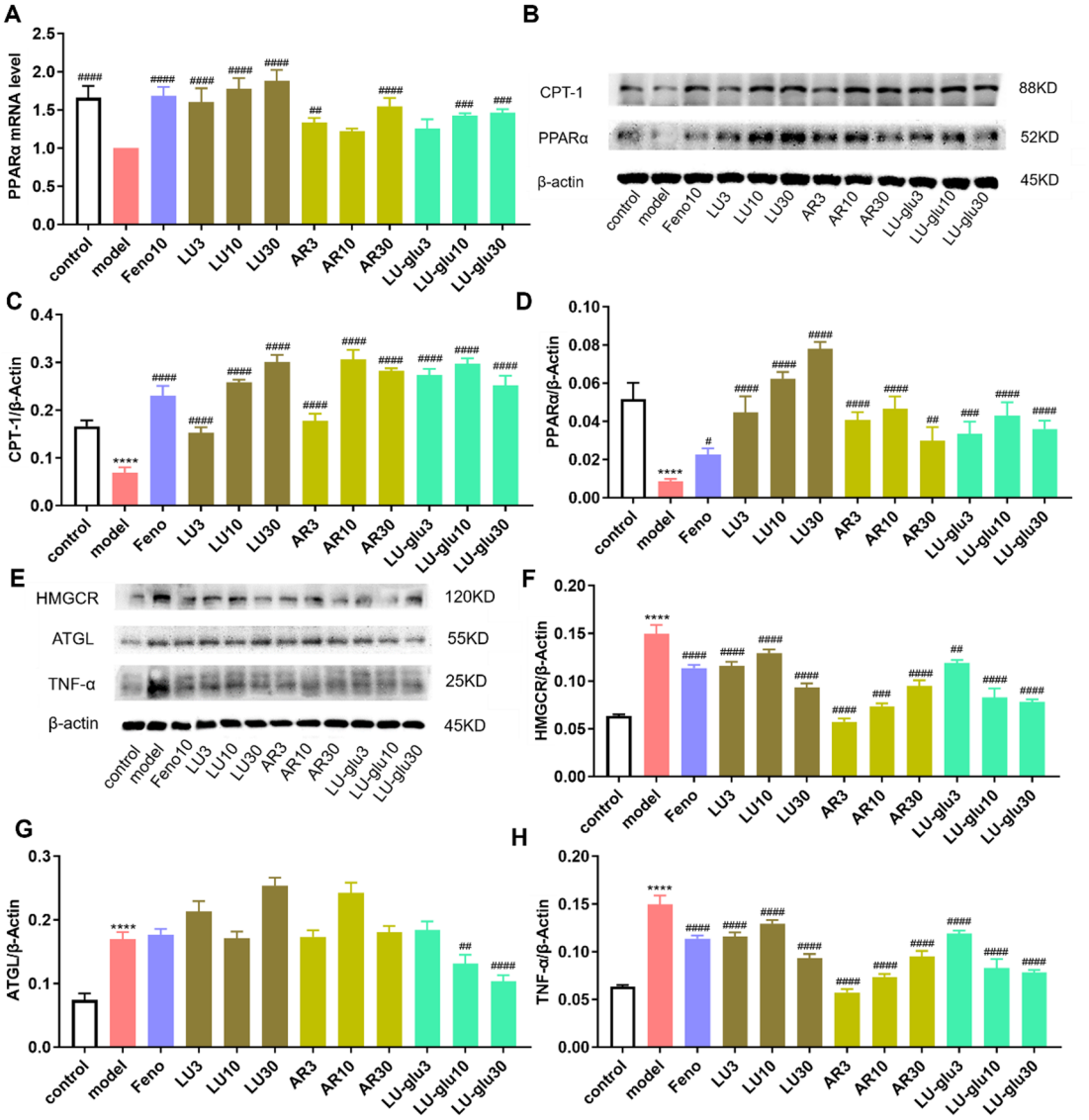

Fig. 6. LU, AR and LU-glu improve MAFLD and inhibit deterioration from enhanced oxidation and other aspects. (**A**) RT-qPCR detection of mRNA expression level of PPARα. (**B**–**D**) Western blot detection of Lipid oxidation related protein bands. (**E**–**H**) Western blot detection of other related protein bands of lipid metabolism (compared with normal group: $^{*}P<0.05$, $^{**}P<0.01$, $^{***}P<0.001$, $^{****}P<0.0001$; compared with model group: $^{\#}P<0.05$, $^{\#\#}P<0.01$, $^{\#\#\#}P<0.001$, $^{\#\#\#\#}P<0.001$).

with the pronounced reduction in TG levels observed following LU-glu treatment, in addition, LU, AR and LU-glu contributed significantly to the down-regulation of the expression of the rate-limiting enzyme of the cholesterol synthesis pathway, HMGCR (Fig. 6E, F), which is favorable for the reduction of cholesterol levels.

In terms of other factors, TNF-α (Fig. 6E, H) was activated in an in vitro model of MAFLD under the induction of FFAs, and when fat accumulated in MAFLD, the inflammatory-related expression of TNF-α increased, which contributed to the progression of MAFLD to more severe NASH. LU, AR, and LU-glu significantly reduced the expression of TNF-α, which effectively curbed the potential inflammation caused by lipid accumulation in an in vitro model of MAFLD. LU, AR and LU-glu significantly reduced the expression of TNF-α and effectively suppressed the potential inflammation induced by lipid accumulation in the MAFLD in vitro model.

Discussion

In this experiment, an in vivo and ex vivo dual model was established to simulate the human disease state as closely as possible to better study the pathopharmacology and pharmacology associated with human diseases and to provide a safer and more solid foundation for the later clinical stage. In the in vivo model, the intervention of CM ethanol total extract in HFD-fed mice resulted in lower body weight, controlled body weight growth rate, weakened steatosis, effective removal of TG, TC and LDL-C from serum, and elevated HDL-C. CM ethanol total extract exhibited significant lipid-lowering activity in the MAFLD mouse model in a concentration- and time-dependent manner.

We carried out a deeper validation in vitro, after intervening the MAFLD in vitro model with different concentrations of total CM ethanol extracts, TG was significantly reduced up to 31% and intracellular lipid droplets were significantly reduced when the concentration of CM reached 20 μg/mL, which confirmed that the total CM ethanol extracts had significant lipid-lowering activity in MAFLD with in vitro. Next, we intervened the in vitro model using single compounds in CM, and found that the four single compounds, LU, AR, LU-glu, and SA, reduced TG by 40%, 43%, 50%, and 61%, respectively, and decreased intracellular lipid accumulation, which was further verified with different concentrations of LU, AR, LU-glu, which were the three compounds with lipid-lowering activity, and cellular TG content was determined, as a result, all the above three compounds showed significant lipid-lowering activity. The relationship between the drugs and their monomers with MAFLD was further verified by RT-qPCR and Western blot methods to verify the effects of the three on lipid metabolism-related proteins and tumor necrosis factor, etc.

The core pathological feature of MAFLD is the imbalance of lipid metabolism in hepatocytes, which is mainly manifested by excessive fatty acid synthesis and insufficient oxidative catabolism. Among them, the SREBP-1c/FAS/ACCα pathway and the PPARα/CPT-1 pathway play a central role in the development of MAFLD as the key regulators of lipid synthesis and oxidative catabolism, respectively[38]. The SREBP-1c/FAS/ACCα pathway serves as a core pathway to promote lipid synthesis, and SREBP-1c is the regulatory fatty acid synthesis key transcription factor[39]. In MAFLD, high-fat diet or insulin resistance activates the expression of SREBP-1c, which in turn upregulates its downstream target genes, FAS and ACCα, and promotes ab initio synthesis of fatty acids. PPARα/CPT-1 pathway as a core pathway to promote lipid synthesis, and PPARα is a key transcription factor that regulates fatty acid oxidation[40]. Its activation upregulates CPT-1 and promotes fatty acid entry from the cytoplasm into the mitochondria for β-oxidation, thereby reducing intrahepatic lipid accumulation. Studies have shown that expectorant formula and lemon bitters significantly ameliorated HFD-induced hepatic steatosis and insulin resistance by activating the PPARα/CPT-1 pathway, and that the coexistence of overactivation of the SREBP-1c/FAS/ACCα pathway and functional inhibition of the PPARα/CPT-1 pathway is a core pathologic feature of MAFLD.

The lipid-lowering mechanism of action of LU, firstly, in terms of lipid synthesis, down-regulates the SREBP-1c/ACCα pathway and reduces the synthesis of fat from scratch; secondly, in terms of lipid oxidation, it enhances lipid oxidation and reduces the accumulation of fat by up-regulating the PPARα/CPT-1 pathway; moreover, muxin reduces the expression of HMGCR, which is beneficial to the reduction of cholesterol level. The lipid-lowering mechanism of action of AR down-regulated the SREBP-1c/ACCα/FAS pathway to reduce intracellular de novo fat in hepatocytes; it likewise up-regulated the PPARα/CPT-1 pathway to enhance lipid oxidation metabolism; and AR also inhibited the expression of HMGCR. The lipid-lowering mechanism of LU-glu was to reduce fat synthesis by inhibiting the SREBP-1c/ACCα/FAS pathway; meanwhile, it down-regulated the lipid oxidation-related PPARα/CPT-1 pathway to metabolically regulate lipid accumulation from both production and oxidation, and to reduce the level of HMGCR to inhibit cholesterol synthesis; in addition, unlike the mechanisms of the other two monomeric compounds, LU-glu uniquely reduced ATGL expression. As the rate-limiting enzyme of triglyceride hydrolysis, ATGL exhibited a compensatory upregulation upon LU-glu treatment, which could modulate ATGL expression and its associated regulatory mechanisms, thereby restoring the TG hydrolysis pathway. This is consistent with the observation that LU-glu achieved the most pronounced TG-lowering effect among the screened compounds, with a reduction rate of 50%.

The three compounds, LU, AR, and LU-glu, also significantly down-regulated the expression of TNF-α, inhibited the underlying inflammation caused by lipid accumulation in MAFLD, and controlled the deterioration of MAFLD to NASH.

One limitation of the present study is the lack of control groups receiving regular chow supplemented with low or high doses of CM extract. This limitation narrows the scope of interpretation, as it does not allow us to clearly distinguish between the intrinsic effects of CM and its interactions with HFD, nor to evaluate the potential effects of CM under non-stressed metabolic conditions. Nonetheless, the present findings provide important insights into the role of CM in HFD-induced metabolic disturbances. In future work, we plan to include such control groups to more comprehensively clarify the mechanisms of action and safety profile of CM, thereby advancing our understanding of its potential applications.

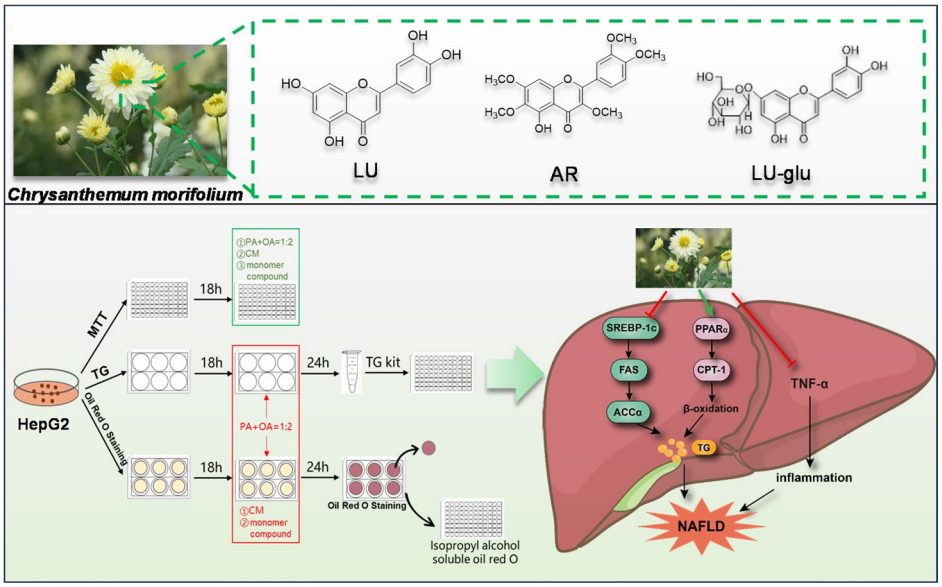

Fig. 7. The monomer compounds with lipid-lowering activity in CM are mainly from the SREBP-1c/FAS/ACCα pathway to reduce lipid synthesis and PPARα/CPT-1 to enhance oxidative improvement in MAFLD, and down-regulate the expression of TNF-α to inhibit the potential inflammation caused by lipid accumulation in MAFLD.

Conclusion

The monomer compounds LU, AR, and LU-glu with lipid-lowering activity in CM intervene mainly from both SREBP-1c/FAS/ACCα and PPARα/CPT-1 pathways to reduce lipid synthesis and enhance oxidation at the same time, which provides a rationale for the utilization of the SREBP-1c/FAS/ACCα and PPARα/ CPT-1 signaling pathways as a target for the treatment of MAFLD. It also provides a basic reference for the development of lipid-lowering active ingredients in CM and further research on their lipid-lowering mechanism (Fig. 7).

Data availability

Data is provided within the manuscript or supplementary information files.

Received: 24 June 2025; Accepted: 27 October 2025
Published online: 17 November 2025

References

1. Eslam, M. et al. The Asian Pacific association for the study of the liver clinical practice guidelines for the diagnosis and management of metabolic dysfunction-associated fatty liver disease. *Hepatol. Int.* **19**, 261–301 (2025).
2. Yang, J-M. et al. Regulatory effect of a Chinese herbal medicine formula on non-alcoholic fatty liver disease. *World J. Gastroenterol.* **25**, 5105–5119 (2019).
3. Wang, Y. et al. Quantitative proteomics analysis based on tandem mass Tag labeling coupled with labeling coupled with liquid chromatography-tandem mass spectrometry discovers the effect of Silibinin on non-alcoholic fatty liver disease in mice. *Bioengineered* **13**, 6750–6766 (2022).
4. Bettini, S. et al. Association of obstructive sleep apnea with non-alcoholic fatty liver disease in patients with obesity: an observational study. *Eat. Weight Disord.* **27**, 335–343 (2022).
5. Wang, Q. et al. Naringenin attenuates non-alcoholic fatty liver disease by down-regulating the NLRP3/NF-κB pathway in mice. *Br. J. Pharmacol.* **177**, 1806–1821 (2020).
6. Chang, B., Baosen, L. I. & Zou, Z. An excerpt of EASL-EASD-EASO clinical practice guidelines for the management of non-alcoholic fatty liver disease. *Linchuang Gandanbing Zazhi 2016*, **32** :1450–1454
7. Yu, D. et al. Higher dietary choline intake is associated with lower risk of nonalcoholic fatty liver in normal-weight Chinese women. *J. Nutr.* **144**, 2034–2040 (2014).
8. Chaves Filho, G. P., Batista, L. A. N. C., de Medeiros, S. R. B., Rocha, H. A. O. & Moreira, S. M. G. Sulfated glucan from the green seaweed *Caulerpa sertularioides* inhibits adipogenesis through suppression of adipogenic and lipogenic key factors. *Mar. Drugs.* **20**, 470 (2022).
9. Nascimento, M. T. et al. Pioglitazone, a peroxisome Proliferator-Activated Receptor-γ Agonist, downregulates the inflammatory response in cutaneous leishmaniasis patients without interfering in *Leishmania Braziliensis* killing by monocytes. *Front. Cell. Infect. Microbiol.* **12**, 884237 (2022).
10. Li, D., Yeung, S-C-J., Hassan, M. M., Konopleva, M. & Abbruzzese, J. L. Antidiabetic therapies affect risk of pancreatic cancer. *Gastroenterology* **137**, 482–488 (2009).
11. Said, A. & Akhter, A. Meta-Analysis of randomized controlled trials of Pharmacologic agents in Non-alcoholic steatohepatitis. *Ann. Hepatol.* **16**, 538–547 (2017).
12. Hannah, W. N. & Harrison, S. A. Lifestyle and dietary interventions in the management of nonalcoholic fatty liver disease. *Dig. Dis. Sci.* **61**, 1365–1374 (2016).
13. Jiang, G. et al. Hepatoprotective mechanism of *Silybum Marianum* on nonalcoholic fatty liver disease based on network Pharmacology and experimental verification. *Bioengineered* **13**, 5216–5235 (2022).

14. Liu, N., Wang, X., Steer, C. J. & Song, G. MicroRNA-206 promotes the recruitment of CD8$^+$ T cells by driving M1 polarisation of Kupffer cells. *Gut* **71**, 1642–1655 (2022).
15. Pan, X., Queiroz, J. & Hussain, M. M. Nonalcoholic fatty liver disease in CLOCK mutant mice. *J. Clin. Invest.* **130**, 4282–4300 (2020).
16. Zhang, H. et al. B-cell lymphoma 6 alleviates nonalcoholic fatty liver disease in mice through suppression of fatty acid transporter CD36. *Cell. Death Dis.* **13**, 359 (2022).
17. Im, A. R., Yang, W. K., Park, Y. C., Kim, S. H. & Chae, S. Hepatoprotective effects of insect extracts in an animal model of nonalcoholic fatty liver disease. *Nutrients* **10**, 735 (2018).
18. Xie, X. et al. Liangxue Jiedu formula improves psoriasis and dyslipidemia comorbidity *via* PI3K/Akt/mTOR pathway. *Front. Pharmacol.* **12**, 591608 (2021).
19. Berlanga, A., Guiu-Jurado, E., Porras, J. A. & Auguet, T. Molecular pathways in non-alcoholic fatty liver disease. *Clin. Exp. Gastroenterol.* **7**, 221–239 (2014).
20. Wu, Z., Yang, F., Jiang, S., Sun, X. & Xu, J. Induction of liver steatosis in BAP31-Deficient mice burdened with Tunicamycin-Induced Endoplasmic reticulum stress. *Int. J. Mol. Sci.* **19**, 2291 (2018).
21. Esler, W. P. & Bence, K. K. Metabolic targets in nonalcoholic fatty liver disease. *Cell. Mol. Gastroenterol. Hepatol.* **8**, 247–267 (2019).
22. Strand, E. et al. Serum acylcarnitines and risk of cardiovascular death and acute myocardial infarction in patients with stable angina pectoris. *J. Am. Heart Assoc.* ;**6**. (2017).
23. Zhang, X-L. et al. Uncarboxylated osteocalcin ameliorates hepatic glucose and lipid metabolism in KKAy mice via activating insulin signaling pathway. *Acta Pharmacol. Sin.* **41**, 383–393 (2020).
24. Lee, Y. H. et al. .et al. Hepatic MIR20B promotes nonalcoholic fatty liver disease by suppressing PPARA. *Elife* ;**10**:. (2021).
25. Franklin, M. P., Sathyanarayan, A. & Mashek, D. G. Acyl-CoA thioesterase 1 (ACOT1) regulates PPARα to couple fatty acid flux with oxidative capacity during fasting. *Diabetes* **66**, 2112–2123 (2017).
26. Hotamisligil, G. S., Shargill, N. S. & Spiegelman, B. M. Adipose expression of tumor necrosis factor-alpha: direct role in obesity-linked insulin resistance. *Science* **259**, 87–91 (1993).
27. Kern, P. A. et al. The expression of tumor necrosis factor in human adipose tissue. Regulation by obesity, weight loss, and relationship to lipoprotein lipase. *J. Clin. Invest.* **95**, 2111–2119 (1995).
28. Zhang, C. et al. The acute effect of metabolic cofactor supplementation: a potential therapeutic strategy against non-alcoholic fatty liver disease. *Mol. Syst. Biol.* **16**, 9495 (2020).
29. Xie Zhanfang, Z. et al. Progress of research on chemical composition and Pharmacological activity of chrysanthemum. *J. Henan Univ. (Medical Edition)*. **34**, 290–300 (2015).
30. Lei, Y. et al. Lactucin ameliorates FFA-induced steatosis in HepG2 cells by modulating mitochondrial homeostasis through the SIRT1/PGC-1α signaling axis. *Heliyon* **10**, e39890 (2024).
31. Xiao, Q. et al. Ginsenoside Rg1 Ameliorates Palmitic Acid-Induced Hepatic Steatosis and Inflammation in HepG2 Cells via the AMPK/NF-κB Pathway. *Int J Endocrinol* 7514802 (2019). (2019).
32. Kong, D. et al. Curcumin blunts epithelial-mesenchymal transition of hepatocytes to alleviate hepatic fibrosis through regulating oxidative stress and autophagy. *Redox Biol.* **36**, 101600 (2020).
33. Kleiner, D. E. et al. Design and validation of a histological scoring system for nonalcoholic fatty liver disease. *Hepatology* **41**, 1313–1321 (2005).
34. Kuo, A., Lee, M. Y. & Sessa, W. C. Lipid droplet biogenesis and function in the endothelium. *Circ. Res.* **120**, 1289–1297 (2017).
35. Li, T., Guo, W. & Zhou, Z. Adipose triglyceride lipase in hepatic physiology and pathophysiology. *Biomolecules* **12**, 57 (2021).
36. Wang, Y., Kory, N., BasuRay, S., Cohen, J. C. & Hobbs, H. H. PNPLA3, CGI-58, and Inhibition of hepatic triglyceride hydrolysis in mice. *Hepatology* **69**, 2427–2441 (2019).
37. Zhang, G. et al. The vesicular transporter STX11 governs ATGL-mediated hepatic lipolysis and lipophagy. *iScience* **25**, 104085 (2022).
38. Wu, C. et al. Alteration of hepatic nuclear receptor-mediated signaling pathways in hepatitis C virus patients with and without a history of alcohol drinking. *Hepatology* **54**, 1966–1974 (2011).
39. Ye, J. et al. Fucoxanthin attenuates free fatty Acid-Induced nonalcoholic fatty liver disease by regulating lipid Metabolism/Oxidative Stress/Inflammation via the AMPK/Nrf2/TLR4 signaling pathway. *Mar. Drugs.* **20**, 225 (2022).
40. Yang, M. et al. Lipid-Lowering effects of *Inonotus obliquus* polysaccharide in vivo and in vitro. *Foods* **10**, 3085 (2021).

Acknowledgements

The work was supported partially by the Natural Science Foundation of Jilin Province, Jilin, China (Grant No. YDZJ202401148ZYTS, YDZJ202201ZYTS155).

Author contributions

Conceptualization: Wenjing Yu, Jun Qiu. Methodology: Yonghu Chen. Investigation: Jun Qiu. Validation& Data curation: Wenjing Yu, Jun Qiu. Writing - Original Draft: Wenjing Yu; Writing - Review & Editing: Xuezheng Li and Xianhua Che. Supervision: Xuezheng Li; Funding acquisition: Xianhua Che and Xuezheng Li. All authors read and approved the final manuscript.

Declarations

Competing interests

The authors declare no competing interests.

Additional information

Supplementary Information The online version contains supplementary material available at https://doi.org/10.1038/s41598-025-25981-7.

Correspondence and requests for materials should be addressed to X.C. or X.L.